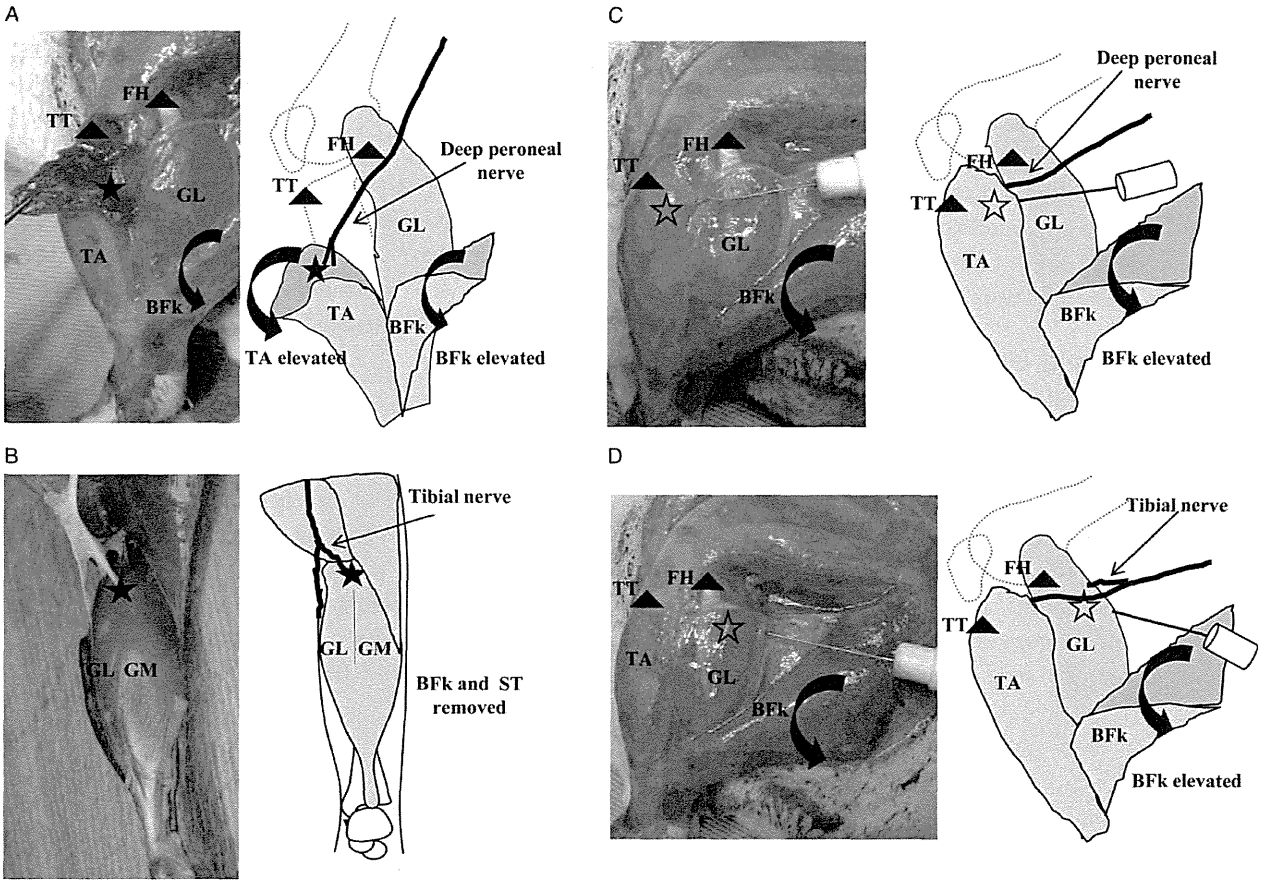

Figure 1 Motor point anatomy of targeted hindlimb muscles and inserting procedures of stimulating electrodes. Detailed motor point anatomy of targeted hindlimb muscles is shown in (A) (TA) and (B) (Gc). In TA (A and C), deep peroneal nerve goes to TA motor point (A ★: 3 mm in depth from the point which is 5 mm below and 5 mm anterior to FH) through just below the fibular head (FH), and it is possible to get the motor point by inserting the needle electrode from just below the FH to TA (C ☆). In Gc (B and D), tibial nerve goes to Gc motor point (B : posterior proximal center of lower hindlimb at level of 5 mm below FH), which is proximal center between GL and GM, at same level of deep peroneal nerve, and it is possible to get the motor point by inserting the needle electrode from the posterior proximal center of the lower hindlimb to GM (D ☆). TA, tibialis anterior; Gc, gastrocnemius; GL, gastrocnemius lateralis; GM, gastrocnemius medialis; ST, semitendinosus; TT, tibial tuberosity; FH, fibular head; BFk, bicepsfemoralis, knee flexion. ★ ☆, motor point; ▲, landmark.

muscles being studied. In this study, twitch threshold currents were determined for different pulse durations (20, 40, 60, 100, 200, and 500 μs).

The rheobase (twitch threshold current at very long pulse duration (here 500 μs) and a range of chronaxie (stimulus duration at the point where the twitch threshold current is twice the rheobase) were determined to assess the excitability of the muscle from the SD curves.

NMES parameters

An isolated four-channel stimulator® (STG2004, Multi Channel Systems, Cytocentrics, Rostock, Germany) was used in this study. In Group A ($n = 5$), the amplitude of the stimulation current was set to 1.5 times the threshold known to produce visual twitches at a pulse width of 40 μs and a frequency of 75 Hz obtained from the SD curves.[23–25] Jung *et al.*[24] reported the rapid ROM decreasing related to muscle fatigue for 15 minutes NMES. Ward and co-workers[26,27] reported the potential usefulness of kHz frequency alternating current for rapid muscle fatigue associated functional electrical stimulation. They[28,29] also reported that a frequency close to 10 kHz is indicated for comfortable motor stimulation, and frequencies above 10 kHz have little or no useful clinical role in rehabilitation procedures. To investigate the usefulness of kHz frequency stimulation for the rapid ROM decreasing related to muscle fatigue, another stimulation pattern with different frequencies and amplitudes was used in this study. In Group B ($n = 5$), the amplitude of the stimulation current was set to three times the threshold known to produce visual twitches at a pulse width of 40 μs and

frequency of 8 kHz (maximum frequency setting in this stimulator system) obtained from the SD curves. The interval between stimulations was set at 0.6 seconds, and the duration of the stimulations was 84 ms at TA and 240 ms at Gc. The timing of the stimulations of the muscles was calibrated in reference to previous electromyogram data obtained from treadmill experiments of normal rats.[30] Stimulations were performed for 15 minutes while the rats were anesthetized.

Three-dimensional kinematic analysis

To evaluate sequential changes in the articular ROM of the stimulated ankle joints, we performed three-dimensional (3D) kinematic analysis using KinemaTracer® (Kissei Comtec Co., Ltd, Nagano, Japan). Colour markers were attached to the joints of both hindlimbs (at the surface of the skin at the iliac region and at the hip, knee, ankle, and metacarpophalangeal joints). Four CCD video cameras were used to film these markers. Using the kinematic analysis software, the ankle joint ROM was calculated and sequential changes were evaluated immediately, 5, 10, and 15 minutes after stimulation (Fig. 2).

Statistical analysis

The paired *t*-test was used to compare sequential changes in ankle ROM and repeated measure analysis of variance was used to compare the two groups. Differences were considered significant based on a hazard ratio of 5% using Excel.

Results

SD curves

Typical SD curves of left TA of Groups A and B were shown in Fig. 3. The curves show a typical nonlinear hyperbolic relationship in which stimulation pulses with shorter pulse widths require higher current amplitude to reach the threshold.

The average rheobase value of each group was calculated to be 0.11 ± 0.06 mA (Group A, $n = 20$) and

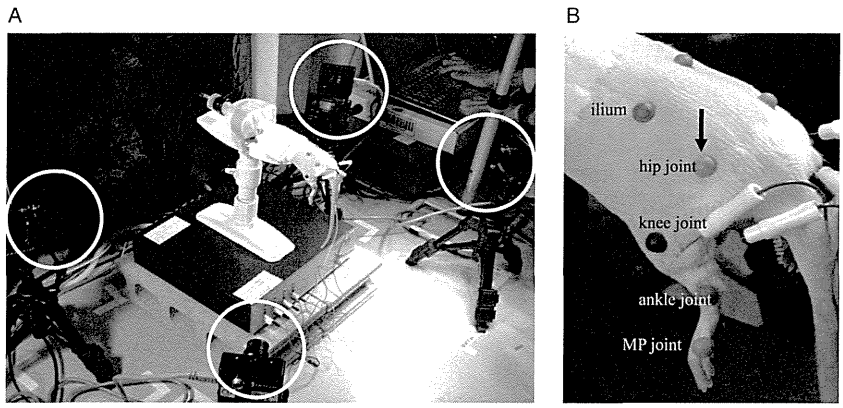

Figure 2 3D kinematic analysis. Color markers (↓) (B) were attached to the limbs and photographed using four CCD cameras (○) (A). 3D motion analysis was performed to evaluate sequential changes in ROM of ankle joints of both hindlimbs during stimulations.

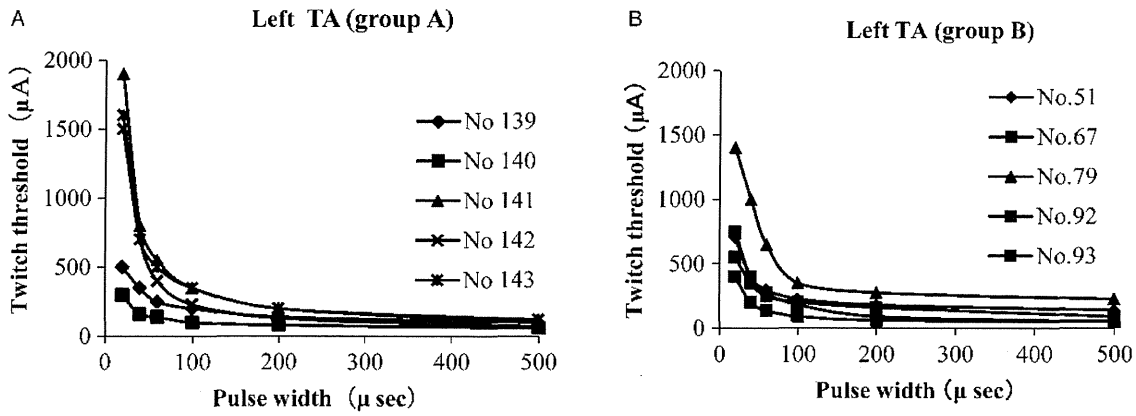

Figure 3 SD curves of left TA muscles of Groups A and B. Typical SD curves of left TA muscles in Groups A (A) and B (B) are shown. Both SD curves show a typical nonlinear hyperbolic relationship in which stimulation pulses with shorter pulse widths require higher current amplitude to reach the threshold.

Table 2 Average rheobase and chronaxie values of each muscle in Groups A and B

	Left TA	Right TA	Left Gc	Right Gc
Group A ($n = 20$)				
Rheobase (mA)	0.9 ± 0.02	1.2 ± 0.05	0.9 ± 0.02	1.5 ± 0.09
Chronaxie (μs)	142 ± 62	120 ± 43	148 ± 54	132 ± 54
Group B ($n = 20$)				
Rheobase	1.1 ± 0.07	2.2 ± 0.1	1.2 ± 0.06	1.7 ± 0.08
Chronaxie	102 ± 56	66 ± 15	72 ± 26	68 ± 8.4

Values are mean ± SE.

0.16 ± 0.03 mA (Group B, $n = 20$), and the average chronaxie value was 135 ± 50 μs (Group A) and 77 ± 33 μs (Group B) (average rheobase and chronaxie values of each muscle are shown in Table 2).

3D kinematic analysis

Fig. 4 shows the sequential changes observed in the average ROM of both ankles of Group A and B rats. The initial average ROM of each group was calculated to be 32 ± 9° for Group A and 61 ± 8° for Group B. In both Groups A and B, a significant decrease in ROM was observed at 5 minutes after the onset of stimuli ($P = 0.001$, Group A; $P = 0.00002$, Group B). In comparison with Group A, ROM of Group B was significantly larger ($P = 0.0006$) at all time points measured, and an interaction between stimulation parameters and period after stimulation ($P = 0.001$) was observed. Fig. 5 shows the stick figure and the average angles of the ankle joints of Group A rat during one stimulation cycle (100%). From the ankle joint paths, we confirmed a joint movement during walking at the timing of walking stimulation.

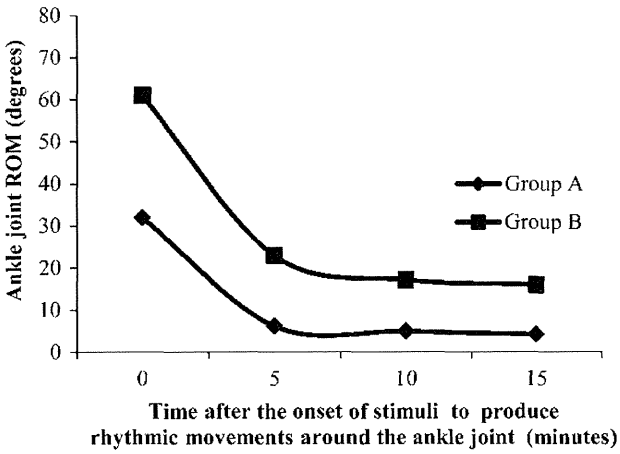

Figure 4 Sequential changes in average ankle joint ROM (Groups A and B). In both Groups A and B, a significant decrease in ROM was observed at 5 minutes after the onset of stimuli. In comparison with Group A, ROM of Group B was significantly larger ($P = 0.0006$) at all time points measured, and an interaction between stimulation parameters and period after stimulation ($P = 0.001$) was observed.

Discussion

To our knowledge, this is the first study to use needle electrodes applicable to rhythmic electrical stimulation of muscles for motor therapy in rats. A problem that emerges when performing NMES with needle electrodes is the placement of electrodes near the motor points of the target muscles. Stimulation sites closer to the motor point require lower charge levels for muscle activation. Ichihara *et al.*[23] reported detailed anatomical motor points of rat hindlimb muscles. The motor points of TA and Gc are relatively easy to stimulate with needle electrodes, and thus were used in this study (Fig. 1). Crago *et al.*[31] reported that the rheobase was 5.2 mA and the chronaxie 85 μs for intramuscular electrodes implanted in the TA of the cat; for electrodes implanted near the peroneal nerve, the rheobase was identified to be 0.38 mA and chronaxie 55 μs. In studies of intramuscular electrodes implanted in rat hindlimb muscles, the rheobase was reported to be 0.16 mA and the chronaxie values ranged from 40 to 90 μs. In this study, we were able to achieve low rheobase currents (0.11 mA, Group A; 0.16 mA, Group B). The average chronaxie value of Group A (135 μs) was higher than Group B (77 μs), that would be attributable to the higher stimulus frequencies of Group B. From these data, we confirmed that the stimulation electrodes were inserted at the appropriate sites near the motor points (Table 2, Fig. 3).

Rhythmic exercises like locomotion can improve motor function in cerebral infarction[14] or spinal cord injury,[15] and electrical stimulation could modify spinal and cortical neural circuitry.[18] To generate locomotor-type movement patterns by electrical stimulation, it is necessary to obtain sufficient angular excursion during electrically stimulated movements. The ROM (flexion plus extension) of the ankle joint was reported to be approximately 65° in 3D kinematic analysis during treadmill walking for rats.[30] Ichihara *et al.*[23] reported that they were able to achieve a total excursion of 70° at ankle joint (35° for flexion and 35 for extension) using NMES (multiple pulse stimulation at 100 Hz, pulse widths of 40 μs, and current amplitude of 1.5

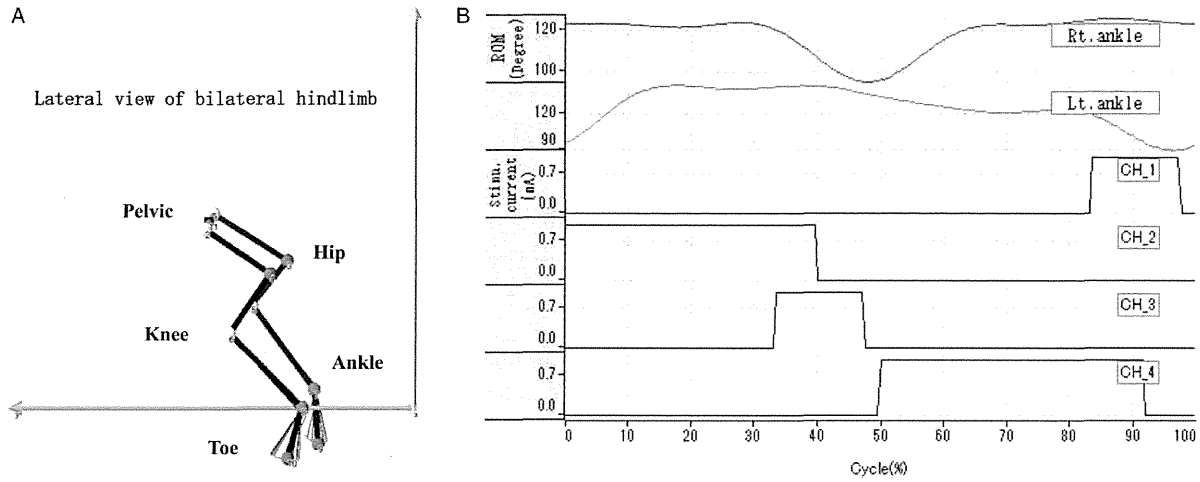

Figure 5 Stick figure and paths of average ankle joint angles on both sides during stimulation The graph (B) shows (Group A, rat no. 143) one cycle of stimulation (100%) immediately after stimulation and the average angle paths of both ankle joints for 11 seconds captures on CCD cameras. The upper two graphs show the paths of the ankle joint angles (the top shows the right ankle joint angle; the second from the top shows the left ankle joint angle) and the bottom four graphs show the stimulation timings and current strengths (CH_1: left TA; CH_2: left Gc; CH_3: right TA; and CH_4; right Gc). The graphs show that good walking joint movement was obtained from the timing of the walking stimulation of both the left and right ankle angle paths. Stick figure (A) shows only ankle joint movement of bilateral hindlimbs during stimulation.

times the twitch threshold current at 40 μs). In this study, the initial average ROM of Group A was relatively small (32 ± 9°), but that of Group B was sufficient for locomotor-type movement of the ankle joint (61 ± 8°). Ankle joint ROM of this study was smaller than that of previous study[23] especially in Group A, because they stimulated each muscle once about 2.5 seconds and calculated each joint ROM which was not rhythmic stimulation of ankle muscle pairs in this study.

Jung *et al.*[24] observed that when using intramuscular electrodes in hip joint agonists, ROM decreases significantly within a minute of stimulation. In this study, we performed electrical stimulation of muscles under stimulation parameters identical to those used by Jung *et al.*[24] While this study was successfully able to utilize cyclic electrical stimulation using needle electrodes in different muscles (Fig. 5), ROM significantly decreased at 5 minutes after stimulation (Fig. 4). Because this was an open-loop stimulation, it was assumed that the stimulated muscles would fatigue.

In previous studies,[32,33] higher intensity and frequency generate stronger muscle contraction, but also a stronger decline in force and thus quick setting muscle fatigue; nevertheless, most of them were based on the results from continuous electrical stimulation. There were several reports on the study of intermittent electrical stimulation.[34–36] Matsunaga *et al.*[35] and Shimada *et al.*[36] showed that high-frequency electrical stimulation elicits less fatigue than low-frequency electrical stimulation during a repetitive stimulation protocol. Dreibati *et al.*[34] reported that only high-frequency (100 Hz) intermittent electrical stimulation within 5 minutes met the criteria of appropriate muscle force training. Ward and co-workers[26,27] reported the potential usefulness of kHz frequency alternating current for rapid muscle fatigue associated functional electrical stimulation. They[28,29] also reported that a frequency close to 10 kHz is indicated for maximum comfort with low torque, and a frequency of 1 kHz or less is preferable for maximum torque.

To assess the impact of electrical stimulation frequency and intensity on muscle force and fatigue, the amplitude of the stimulation current was set to three times the threshold known to produce visual twitches at a pulse width of 40 μs and frequency of 8 kHz. A significant decrease in ROM was observed at 5 minutes after stimulation in Group B, but in comparison with Group A ROM was larger in Group B at all time points ($P = 0.0006$) (Fig. 5). ROM was maintained in Group B, and based on the fact that interactions exist between the stimulus parameters and period after stimulation ($P = 0.001$), it can be inferred that it is possible to counteract decreases in ROM due to muscle fatigue by using high-amplitude and high-frequency stimulation currents within 15 minutes in this study. Therefore, it is possible to maintain ROM by using a stimulus program in which both frequency and current are increased incrementally during stimulation. Nevertheless, stimulation frequency used in Group B is very high (8 kHz), and there is no report of kHz frequency electrical stimulation

for locomotor training. It is essential, therefore, to identify appropriate frequency and amplitude of NMES to counteract muscle fatigue in the future.

Other methods for maintaining ROM have also been previously reported. Fairchild *et al.*[37] successfully utilized adaptive NMES with intramuscular electrodes embedded in the hip joint of rats with spinal cord injuries.[37] They used a pattern generator/pattern shaper closed-loop stimulator – which maintains ROM by using real-time feedback of the hip joint angle during stimulation to set the ideal hip joint motion path in advance – to automatically adjust the current pulse amplitude and correct errors. Using this type of stimulation algorithms in the future should be able to solve the problem of muscle fatigue encountered in this study. As potential limitations of this electrical stimulation of muscles for motor therapy, the movements produced by the stimulation of only ankle joint muscles cannot provide a replacement for locomotion involving all of the muscles normally active during walking movements. The combination therapy, such as body weight support treadmill training, could be necessary for more effective functional recovery.[4] The needle electrodes used in this study cannot replace surface electrodes as clinical NMES application (Table 1), but the needle electrode could have a potential usefulness as a tool for peripheral nerve stimulation, that may modulate plasticity in the spinal cord.[7,16,38]

Conclusion

In summary, a less invasive muscular electrical stimulation model for motor therapy was developed using needle electrodes. SD curves were used to confirm that the stimulation electrodes were inserted at the appropriate sites. Rhythmic stimulation of the leg joints using muscular electrical stimulation with needle electrodes was successful, but evaluation of sequential ROM using 3D kinematic analysis showed that at 5 minutes after stimulation, a significant decrease in ROM was observed. High-frequency and high-amplitude stimulation was also shown to be effective in alleviating decreases in ROM due to muscle fatigue. In comparison with NMES therapy rodent models that use intramuscular electrodes, this model is less invasive and can be used in combination with spinal regeneration therapies from the acute stage.

References

1 Raineteau O, Schwab M. Plasticity of motor systems after incomplete spinal cord injury. Nat Rev Neurosci 2001;2(4):263–73.
2 Ramer LM, Ramer MS, Steeves JD. Setting the stage for functional repair of spinal cord injuries: a cast of thousands. Spinal Cord 2005;43(3):134–61.
3 Barbeau H, McCrea DA, O'Donovan MJ, Rossignol S, Grill WM, Lemay MA. Tapping into spinal circuits to restore motor function. Brain Res Rev 1999;30(1):27–51.
4 Field-Fote EC. Combined use of body weight support, functional electric stimulation, and treadmill training to improve walking ability in individuals with chronic incomplete spinal cord injury. Arch Phys Med Rehabil 2001;82(6):818–24.
5 Wirz M, Zemon DH, Rupp R, Scheel A, Colombo G, Dietz V, *et al.* Effectiveness of automated locomotor training in patients with chronic incomplete spinal cord injury: a multicenter trial. Arch Phys Med Rehabil 2005;86(4):672–80.
6 De Leon R, Hodson J, Roy R, Edgerton V. Locomotor capacity attributable to step training versus spontaneous recovery after spinalization in adult cats. J Neurophysiol 1998;79(3): 1329–40.
7 Rossignol S, Barriere G, Frigon A, Barthelemy D, Bouyer L, Provencher J, *et al.* Plasticity sensorimotor interactios after peripheral and/or spinal lesions. Brain Res Rev 2008;57(1):228–40.
8 Keith MW. Neuroprostheses for the upper extremity. Microsurgery 2001;21(6):256–63.
9 Peckham PH, Keith MW, Kilgore KL, Grill JH, Wuolle KS, Thrope GB, *et al.* Efficacy of an implanted neuroprosthesis for restoring hand grasp in tetraplegia: a multicenter study. Arch Phys Med Rehabil 2001;82(10):1380–8.
10 Snoek GJ, Ijzerman MJ, in 't Groen FA, Stoffers TS, Zilvold G. Use of the NESS handmaster to restore hand function in tetraplegia: clinical experiences in ten patients. Spinal Cord 2000;38(4):244–9.
11 Hendricks HT, Ijzerman MJ, de Kroon JR, in 't Groen FA, Zilvold G. Functional electrical stimulation by means of the 'Ness Handmaster Orthosis' in chronic stroke patients: an exploratory study. Clin Rehabil 2001;15(2):217–20.
12 Ring H, Rosenthal N. Controlled study of neuroprosthetic functional electrical stimulation in sub-acute post-stroke rehabilitation. J Rehabil Med 2005;37(1):32–6.
13 Field-Fote EC, Tepavac D. Improved intralimb coordination in people with incomplete spinal cord injury following training with body weight support and electrical stimulation. Phys Ther 2002; 82(7):707–15.
14 Beekhuizen KS, Field-Fote EC. Massed practice versus massed practice with stimulation: effects on upper extremity function and cortical plasticity in individuals with incomplete cervical spinal cord injury. Neurorehabil Neural Repair 2005;19(1):33–45.
15 Popovic MR, Thrasher TA, Adams ME, Takes V, Zivanovic V, Tonack MI. Functional electrical therapy: retraining grasping in spinal cord injury. Spinal Cord 2006;44(3):143–51.
16 Nudo RJ, Milliken GW, Jenkins WM, Merzenich MM. Use-dependent alterations of movement representations in primary motor cortex of adult squirrel monkeys. J Neurosci 1996;16(2): 785–807.
17 Liepert J, Bauder H, Wolfgang HR, Miltner WH, Taub E, Weiller C. Treatment-induced cortical reorganization after stroke in humans. Stroke 2000;31(6):1210–6.
18 Field-Fote EC. Electrical stimulation modifies spinal and cortical neural circuitry. Exerc Sport Sci Rev 2004;32(4):155–60.
19 Bouyer LJ. Animal models for studying potential training strategies in persons with spinal cord injury. J Neurol Phys Ther 2005;29(3):117–25.
20 Edgerton VR, Roy RR. Robotic training and spinal cord plasticity. Brain Res Bull 2009;78(1):4–12.
21 Courtine G, Gerasimenko Y, van den Brand R, Yew A, Musienko P, Zhong H, *et al.* Transformation of non-functional spinal circuits into functional states after the loss of brain input. Nat Neurosci 2009;12(10):1333–42.
22 Jung R, Ichihara K, Venkatasubramanian G, Abbas JJ. Chronic neuromuscular electrical stimulation of paralyzed hindlimbs in a rodent model. J Neurosci Methods 2009;183(2):241–54.
23 Ichihara K, Venkatasubramanian G, Abbas JJ, Jung R. Neuromuscular electrical stimulation of the hindlimb muscles for movement therapy in a rodent model. J Neurosci Methods 2009; 176(2):213–24.
24 Jung R, Belanger A, Kanchiku T, Fairchild M, Abbas JJ. Neuromuscular stimulation therapy after incomplete spinal cord injury promotes recovery of interlimb coordination during locomotion. J Neural Eng 2009;6(5):055010. Epub.

25 Kanchiku T, Lynskey JV, Protas D, Abbas JJ, Jung R. Neuromuscular electrical stimulation induced forelimb movement in a rodent model. J Neurosci Methods 2008;167(2): 317–26.
26 Ward AR. Electrical stimulation using kilohertz frequency alternating current. Phys Ther 2009;89(2):181–90.
27 Ward AR, Robertson VJ. The variation in fatigue rate with frequency using kHz frequency alternating current. Med Eng Phys 2000;22(9):637–46.
28 Ward AR, Robertson VJ. Variation in torque production with frequency using medium frequency alteration current. Arch Phys Med Rehabil 1998;79(11):1399–404.
29 Ward AR, Robertson VJ. Variation in motor threshold with frequency using kHz frequency alternating current. Muscle Nerve 2001;24(10):1303–11.
30 Thota AK, Watson SC, Knapp E, Thompson B, Jung R. Neuromechanical control of locomotion in the rat. J Neurotrauma 2005;22(4):442–65.
31 Crago PE, Peckham PH, Mortimer JT, Van der Meulen JP. The choice of pulse duration for chronic electrical stimulation via surface, nerve, and intramuscular electrodes. Ann Biomed Eng 1974;2(3):252–64.
32 Edwards RHT, Young A, Hosking GP, Jones DA. Human skeletal muscle function: description of tests and normal values. Clin Sci Mol Med 1977;52(3):283–90.
33 Jones DA, Bigland-Ritchie B, Edwards RH. Excitation frequency and muscle fatigue: mechanical responses during voluntary and stimulated contractions. Exp Neurol 1979;64(2):401–13.
34 Dreibati B, Lavet C, Pinti A, Poumarat G. Influence of electrical stimulation frequency on skeletal muscle force and fatigue. Ann Phys Rehabil Med 2010;53(4):266–77.
35 Matsunaga T, Shimada Y, Sato K. Muscle fatigue from intermittent stimulation with low and high frequency electrical pulses. Arch Phys Med Rehabil 1999;80(1):48–53.
36 Shimada Y, Ito H, Matsunaga T, Misawa A, Kawatani M, Itoi E. Reduction of muscle fatigue by catchlike-inducing intermittent electrical stimulation in rat skeletal muscle. Biomed Res 2006;27(4):183–9.
37 Fairchild MD, Kim SJ, Iarkov A, Abbas JJ, Jung R. Repetitive hindlimb movement using intermittent adaptive neuromuscular electrical stimulation in an incomplete spinal cord injury rodent model. Exp Neurol 2010;223(2):623–33.
38 Asensio-Pinilla E, Udina E, Jaramillo J, Navatto X. Electrical stimulation combined with exercise increase axonal regeneration after peripheral nerve injury. Exp Neurol 2009;219(1):258–65.

Research article

Biomechanical analysis of cervical spondylotic myelopathy: The influence of dynamic factors and morphometry of the spinal cord

Norihiro Nishida[1], Yoshihiko Kato[1], Yasuaki Imajo[1], Syunichi Kawano[2], Toshihiko Taguchi[1]

[1]Yamaguchi University Graduate School of Medicine, Yamaguchi University, Japan, [2]Faculty of Engineering, Yamaguchi University, Japan

Objective: Patients with cervical spondylotic myelopathy (CSM) have the same clinical symptoms that vary according to the degree of spinal cord compression and the cross-sectional cord shape. We used a three-dimensional finite element method (3D-FEM) to analyze the stress distributions of the spinal cord with neck extension under three cross-sectional cord shapes.
Methods: Experimental condition for the 3D-FEM spinal cord, ligamentum flavum, and anterior compression shape (central, lateral, and diffuse types) was established. To simulate neck extension, the spinal cord was extended by 20° and the ligamentum flavum was shifted distally according to movement of the cephalad lamina.
Results: The stress distribution in the spinal cord increased due to invagination of the ligamentum flavum into the neck extension. The range of stress distribution observed for the diffuse type was wider than for the central and lateral types. In addition, the stress distribution in the spinal cord was increased by the pincer movement of the ligamentum flavum and by the anterior compression of the spinal cord. The range of stress distribution observed for the diffuse type under antero-posterior compression was also wider than for the central and lateral types.
Conclusion: This simulation model showed that the clinical symptoms of CSM due to compression of the diffuse type may be stronger than for the central and lateral types. Therefore, careful follow-up is recommended for anterior compression of the spinal cord of diffuse type.

Keywords: Spinal cord, Morphometry, Cervical spondylotic myelopathy, Finite element method, Ligamentum flavum, Pincer effect, Spinal cord, Anterior compression

Introduction

The number of patients with cervical spondylotic myelopathy (CSM) is increasing due to the aging population. The neurologic dysfunction may initially be mild and associated with minimal disability; however, progressive spinal cord compression can lead to severe neurologic deterioration major disability. CSM manifests itself following static or dynamic compression of the spinal cord. Static factors include developmental canal stenosis, bulging of the intervertebral disc posterior margin, and hypertrophy of the ligamentum flavum. Dynamic factors include invagination of the ligamentum flavum (buckling) and a pincer effect (anterior and posterior cord impingement)[1,2] during neck extension. Of note, patients with CSM do not necessarily share the same symptoms. These differ according to the degree of spinal cord compression and the cross-sectional cord shape.[3,4] The latter factor was the basis of a study on patients with myelopathy that classified cord morphology according to the deformity.

There have been several reports on the relationship between cross-sectional cord shapes and prognosis.[3–7] The spinal cord shape observed by computed tomography myelography (CTM) or magnetic resonance imaging (MRI) was classified into three general morphological types (central, lateral, and diffuse) by Fujiwara *et al.*[9]

The prognosis for patients with CSM varies according to the morphometry of spinal cord compression. Image-based analyses have been reported; however, so far there are no reports on morphometry-based analysis of stress

Correspondence to: Norihiro Nishida, Yamaguchi University Graduate School of Medicine, Ube, Yamaguchi, 775–850, Japan.
Email: n005uk@yamaguchi-u.ac.jp

DOI 10.1179/2045772312Y.0000000024

distribution. In this study, we used a three-dimensional finite element method (3D-FEM) to analyze the stress distribution in the spinal cord with neck extension and under three anterior compression shapes.

Methods

The ABAQUS 6.11 (Valley Street, Providence, RI, USA) finite element package was used for FEM simulation. The 3D-FEM spinal cord model used in this study consisted of the gray matter, white matter, and pia mater (Fig. 1). In order to simplify calculation in the model, the denticulate ligament, dura, and nerve root sheaths were not included. The pia mater was included as it has been demonstrated that the spinal cord with and without this component shows significantly different mechanical behavior.[8] The spinal cord was assumed to be symmetrical about the mid-sagittal plane, such that only half the spinal cord required reconstruction and the whole model could be integrated by mirror image. The vertical length of the spinal cord for CTM measurement was two vertebral bodies (approximately 80 mm).

The ligamentum flavum model was established by measuring CTM and MRI. In order to simplify calculation in the model, the ligamentum flavum was a linear shape. The angle of the ligamentum flavum was set to open 10° outward from the posterior spinal cord center as deduced from the literature (Fig. 2).[9]

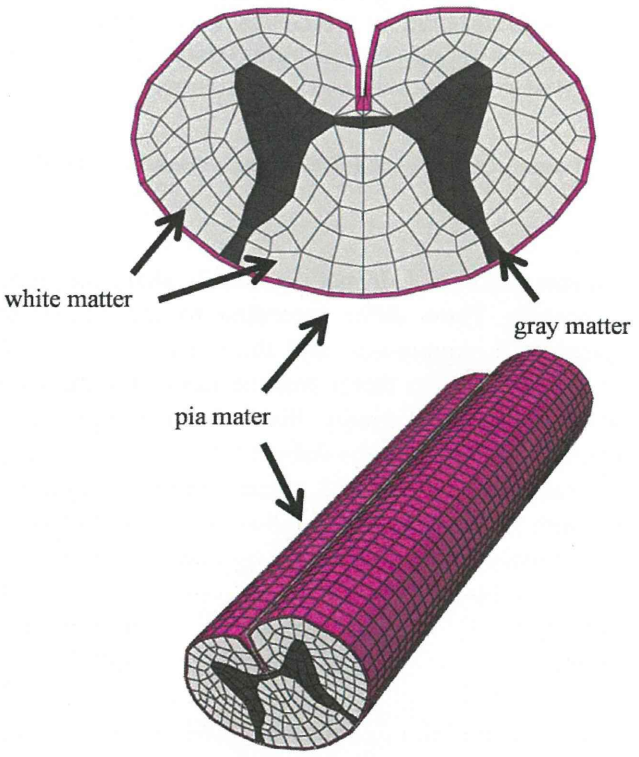

Figure 1 The three-dimensional finite element method model of the spinal cord consisted of the gray matter, white matter, and pia mater.

The shapes resulting from anterior compression on the spinal cord were classified as central, lateral, and diffuse type. A rigid flat plate was used as the compression factor on the anterior surface of the spinal cord for the lateral and diffuse types, while a semi-circular plate was used for the central type. The shape of the semi-circular plate for the central type was deduced from the literature (Fig. 3).[9]

The model simulated CSM under three shapes of anterior compression of the spinal cord, as well as dynamic compression under neck extension of the cervical spinal cord. The rigid flat plate and the semi-circular plate were located at inferior margin of the posterior vertebral body. The ligamentum flavum was located at the anterior surface of the cephalad lamina and at the superior margin of the caudal lamina. The position of the three anterior compression plates and the ligamentum flavum was set according to MRI resulting from the literature.[10]

The spinal cord consists of three distinctive materials referred to as the white matter, gray matter, and pia mater. The mechanical properties (Young's modulus and Poisson's ratio) of the gray and white matter were determined using data obtained by the tensile stress strain curve and stress relaxation under various strain rates.[11,12] The mechanical properties of the pia mater and the ligamentum flavum were obtained from the literature.[13,14] The mechanical properties of the flat plate and semi-circular plate were stiff enough for the spinal cord to be pressed. On the basis of the assumption that no slippage occurs at the interfaces of the white matter, gray matter, and pia mater, these interfaces were glued together. There are no data on the friction coefficient between the ligamentum flavum and the spinal cord. The coefficient of friction between the ligamentum flavum and the spinal cord was frictionless at the contact interfaces and adjacent to the part in contact. Similarly, the coefficient of friction between the rigid flat plate and the spinal cord, or the semi-circular plate and the spinal cord, was frictionless at the contact interfaces and adjacent to the part in contact.

The spinal cord, the rigid flat plate, the semi-circular plate, and the ligamentum flavum model were symmetrically meshed with 20-node elements. With an FEM model for diffuse type of rigid flat plate of the spinal cord, the total number of isoperimetric 20-node elements was 10 104 and the total number of nodes was 57 433.

For the simulation of CSM under neck extension, nodes at the bottom of the spinal cord model were

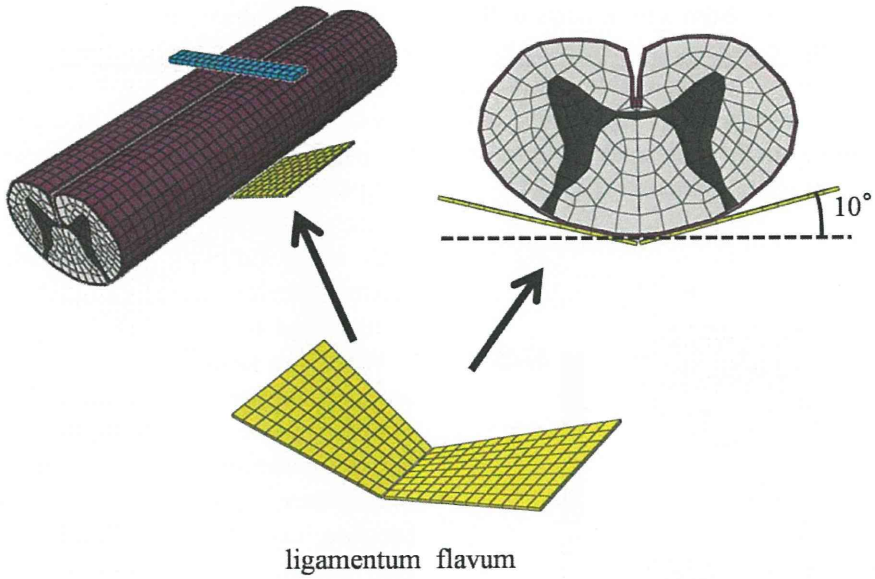

Figure 2 The ligamentum flavum model was established using the rear of the spinal cord.

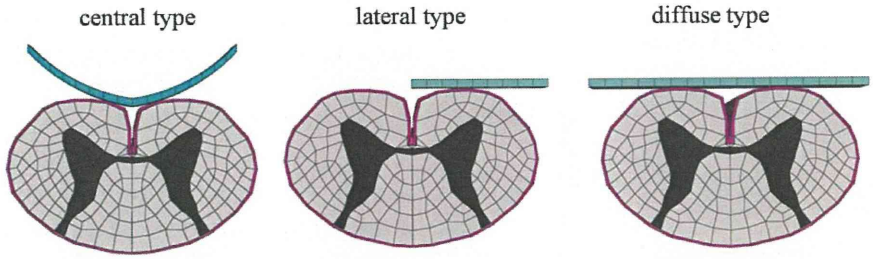

Figure 3 The shapes for anterior compression of the spinal cord were central type, lateral type, and diffuse type.

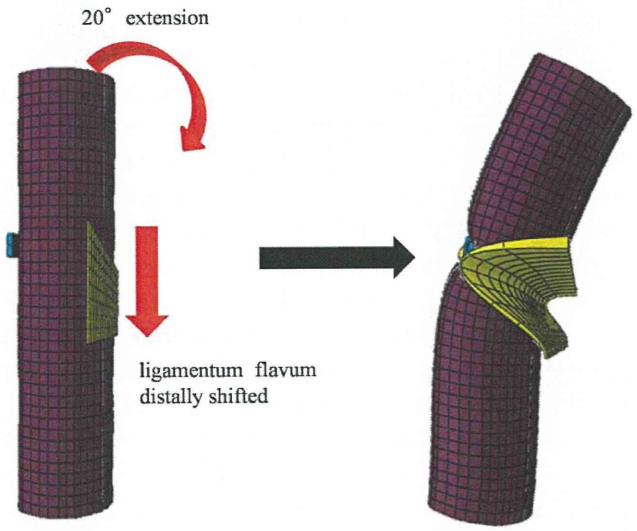

Figure 4 For the simulation of neck extension, an extension of 20° was applied to the spinal cord. The ligamentum flavum moved distally in accordance with movement of the cephalad lamina.

constrained in all directions and the extension angle of the superior margin of the spinal cord was 20°. The flat plate and the semi-circular plate were constrained in all directions. On the basis of assumption that the caudal vertebral body of the responsible lesion in patients with CSM was stable, the bottom of the ligamentum flavum was constrained in all directions. The superior margin of the ligamentum flavum shifted distally according to the movement of cephalad lamina. The angle of neck extension and the direction in which the ligamentum flavum moved were obtained from each angle of C3–C4 kinematic MRI published by Iwabuchi *et al.*[15] (Fig. 4).

FEM analysis was conducted under each of the above conditions and in duplicate to test the reproducibility of results with this model.

Results

When the shape of the spinal cord resulting from anterior compression was the central type, stress distributions

were observed in the posterior horn and in parts of the posterior funiculus, lateral funiculus, and anterior horn beneath the invagination by the ligamentum flavum. Under antero-posterior compression, high-stress distributions were observed in the gray matter, anterior funiculus, and part of the lateral funiculus (Fig. 5A).

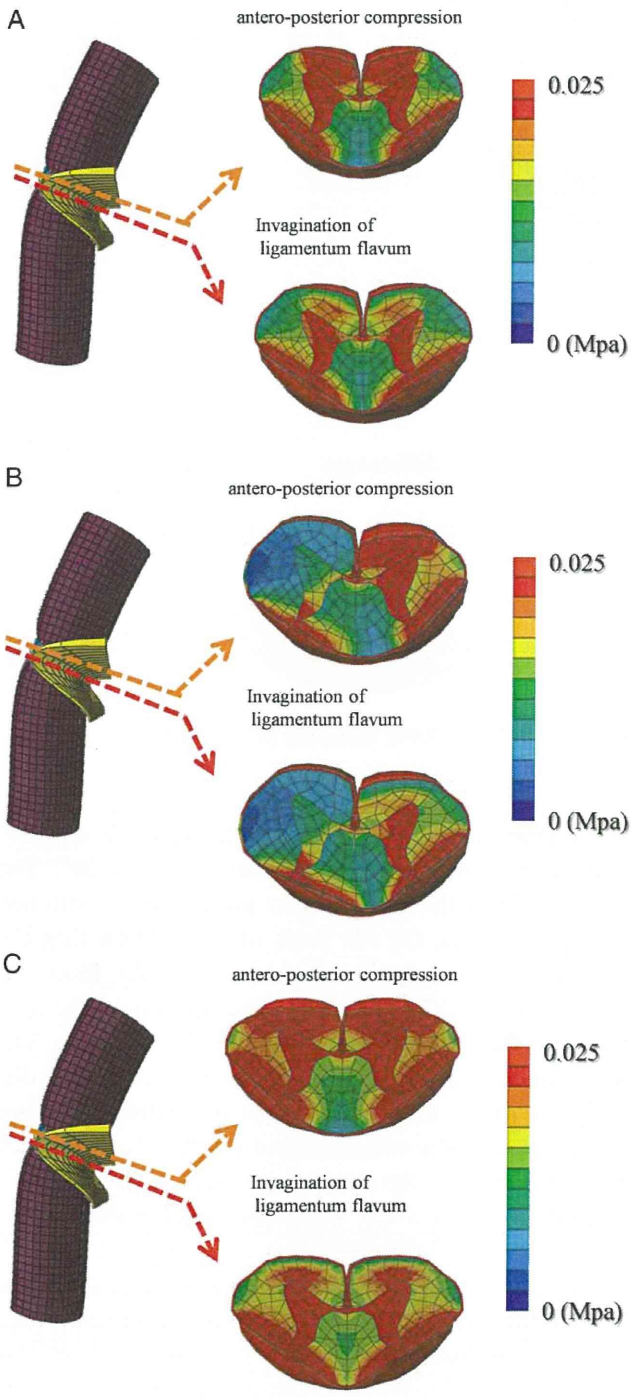

Figure 5 Stress distributions under invagination of the ligamentum flavum and under antero-posterior compression are shown for the central, lateral, and diffuse type shapes following anterior compression of the spinal cord (A–C).

When the shape of the spinal cord resulting from anterior compression was the lateral type, stress distributions were observed in the gray matter and lateral funiculus on the compression side, as well as parts of the posterior funiculus and posterior horn on the non-compression side beneath the invagination by the ligamentum flavum. Under antero-posterior compression, high stress distributions were observed in the gray matter, anterior funiculus, and lateral funiculus on the compression side (Fig. 5B).

When the shape of the spinal cord resulting from anterior compression was the diffuse type, stress distributions were observed in the gray matter, lateral funiculus, and posterior funiculus beneath the invagination by the ligamentum flavum. Under antero-posterior compression, high-stress distributions were observed in the gray matter, anterior funiculus, lateral funiculus, and part of the posterior funiculus (Fig. 5C).

Discussion

CSM is the most common type of spinal cord dysfunction in patients over the age of 55 years, but can sometimes be difficult to recognize. Although it is the most common reason for spinal cord dysfunction in the elderly individuals, CSM has no pathognomonic symptoms or physical signs. Because no single neurologic feature is unique to cervical myelopathy, diagnosis must be established by the affirmation of associated clinical signs and symptoms, in parallel with the exclusion of other clinical entities that may also show these signs.

CSM is a well-described clinical syndrome that can arise due to a combination of etiological factors. This clinical entity manifests itself following static or dynamic compression of the spinal cord, causing compression of the enclosed cord and leading to local tissue ischemia, injury, and neurological impairment. Static factors include developmental canal stenosis, bulging of the intervertebral disc posterior margin, and hypertrophy of the ligamentum flavum. With regard to dynamic factors, the spinal cord of patients with CSM is likely to be compressed during neck extension because of the protrusion of the ligamentum flavum and intervertebral discs into the spinal canal (pincer mechanism).[2] Recent developments in imaging have enabled closer examination of the cervical spine through improved CT and MRI. Using multidetector-row CT, Machino *et al.*[7] reported narrowing of the spinal cord cross-sectional area during neck extension in patients with CSM. In healthy individuals, Muhle *et al.*[16,17] found that the subarachnoid space was smallest at extension compared with its size at mid-position

and at flexion of the cervical spine. These workers also showed an increasing prevalence of functional cord impingement from the posterior aspect and from both the anterior and posterior aspects during neck extension in patients with advancing stages of degenerative disease of the cervical spine.

With regard to morphological changes in the spinal cord, the symptoms of CSM patients differ according to the degree of spinal cord compression and the cross-sectional cord shape. Yu *et al.*[5] reported that the severity of symptoms correlated with the degree of spinal cord deformity. Kameyama *et al.*[3] reported that a triangular-shaped spinal cord was associated with severe and irreversible pathological changes, whereas Shimomura and Washimi[4] found this shape was associated with a more severe prognosis compared with oval-shaped or boomerang-shaped spinal cords. The spinal cord shape was classified into three general morphological types (central, lateral, and diffuse) by Fujiwara *et al.*[9] These investigators reported that the prognosis of CSM patients with the diffuse-type shape was poorer than those with the central or lateral types.

Using this prior knowledge, we investigated whether the morphology of the spinal cord following anterior compression was associated with difference in stress distribution for the same dynamic motion. Our first goal was to develop a 3D-FEM spinal cord model that simulates the clinical situation, whereas our second goal was to analyze the clinical condition of patients. Similar to previous studies by Kato *et al.*,[18–20] Xin-Feng Li *et al.*,[21,22] and Nishida *et al.*,[23] bovine spinal cord was used in the current analytical model as it was impossible to obtain fresh human spinal cord. Xin-Feng *et al.*[21] noted that it was reasonable to use the mechanical properties of bovine spinal cord because the brain and spinal cord of cattle and humans show similar injury changes. For the purpose of this study, we therefore assumed that the mechanical properties of the spinal cord from these two species were similar.

Our study was limited to the investigation of stress distribution caused by compression. Other casual factors that can contribute to CSM include ischemia, congestion, and spinal cord stretch injury.[24] Blood flow was not factored into this FEM analysis and only one movement (neck extension) was investigated for association with CSM. Long-term compression and apoptotic factors were not considered in the FEM analysis. Moreover, the FEM model used here was simplified in order to facilitate the calculations. Analysis errors were reduced by using a FEM mesh, by assuming the spinal cord was symmetric, by not including the denticulate ligament, dura, and nerve root sheaths, and by setting a close distance between the spinal cord and ligamentum flavum, spinal cord and anterior compression of the spinal cord.

In pathology-based studies, Ono *et al.*[25] and Ogino *et al.*[26] described how patients with severe myelopathy had spinal cord atrophy and also presented with extensive degeneration and infarction of the entire gray matter and white columns, except for the anterior funiculus. In this analysis, stress distributions in the anterior funiculus were also increased. However, as this increase is not associated with any clinical symptoms or with apoptosis, the current results merely provide an estimate for the possible range of increased stress distribution at this site. Nevertheless, the observed morphometric pattern was similar to a prior clinical report and hence our results may still be applicable to the clinical situation. More complex materials and structural characteristics of the spinal cord model should be included in future investigations.

In this study, stress distribution in the spinal cord was increased by the invagination of the ligamentum flavum during neck extension. However, the range of stress distributions for the three types of anterior compression of the spinal cord was not uniform (Figs. 5A–5C). The range of stress distribution observed for the diffuse type was wider than for the central and lateral types.

In addition, stress distribution in the spinal cord was increased by the pincer movement of the ligamentum flavum and by anterior compression of the spinal cord. However, in this situation the range of stress distribution for the three types of anterior compression of the spinal cord was not uniform. The range of stress distribution under antero-posterior compression was also wider for the diffuse type compared with the central and lateral types. Moreover, the compressed spinal cord shape with diffuse type was a triangular shape and was supposed to be a severe prognosis.

Conclusion

This simulation model showed that the stress distribution with the diffuse type of compression was wider than with the central and lateral types. The symptoms of CSM associated with diffuse type may therefore be stronger than for CSM with the central or lateral types. We recommend more careful follow-up of anterior compression of the spinal cord when the resultant shape is the diffuse type.

References

1 Taylor AR. Mechanism and treatment of spinal-cord disorders associated with cervical spondylosis. Lancet 1953;1(6763):717–20.
2 Penning L. Some aspects of plain radiography of the cervical spine in chronic myelopathy. Neurology 1962;12:513–9.

3 Kameyama T, Hashizume Y, Ando T, Takahashi A, Yanagi T, Mizuno J. Spinal cord morphology and pathology in ossification of the posterior longitudinal ligament. Brain 1995;118:263–78.
4 Shimomura T, Washimi M. The natural course of cervical spondylotic myelopathy: follow-up of conservative treatment after admission. Rinsho-Seikeigeka 2004;39(4):439–44 (Japan).
5 Yu YL, Stevens JM, Kandall B, du Bourlay GH. Cord shape and measurements in cervical spondylotic myelopathy and radiculopathy. AJNR 1983;4(3):839–42.
6 Hayashi H, Okada K, Hashimoto J, Tada K, Ueno R. Cervical spondylotic myelopathy in the aged patient. A radiographic evaluation of the aging changes in the cervical spine and etiologic factors of myelopathy. Spine 1988;13(6):618–25.
7 Machino M, Yukawa Y, Ito K, Nakashima H, Kato F. Dynamic changes in dural sac and spinal cord cross-sectional area in patients with cervical spondylotic myelopathy. Spine 2011;36(5):399–403.
8 Cecilia P, Jon S, Richard M. The importance of Fluid-Structure Interaction in spinal trauma models. J Neurotrauma 2011;28(1): 113–25.
9 Fijiwara K, Yonenobu K, Hiroshima K, Fuji T, Ehara S, Yamashita K, *et al.* The evaluation of viability of the spinal cord by CT myelography. Rinsho Seikei Geka 1986;21:355–61 (Japan).
10 Tani T, Yamamoto H, Kimura J. Cervical spondylotic myelopathy in elderly people: a high incidence of conduction block at C3-4 or C4-5. J Neural Neurosurg Psychiatry 1999;66(4):456–64.
11 Ichihara K, Taguchi T, Yoshinori S, Ituo S, Shunichi K, Shinya K. Gray matter of the bovine cervical spinal cord is mechanically more rigid and fragile than the white matter. J Neurotrauma 2001;18(3):361–7.
12 Ichihara K, Taguchi T, Sakuramoto I, Kawano S, Kawai S. Mechanism of the spinal cord injury and the cervical spondylotic myelopathy: new approach based on the mechanical features of the spinal cord white and gray matter. J Neurosurg 2003;99(3 suppl.):278–85.
13 Tunturi AR. Elasticity of the spinal cord, pia and denticulate ligament in the dog. J Neurosurg 1978;48(6):975–9.
14 Ueno H, Taguchi T, Toyoda K, Ichihara K, Kawai S, Kawano K. Mechanical characteristic with the aging of the lumbar vertebrae ligamentum flavum. Seikeigeka to Saigaigeka 2002;51(4):367–9 (Japan).
15 Iwabuchi M, Kikuchi S, Yabuki S. Kinematic MRI and preoperative evaluation in cervical spondylotic myelopathy. Rinsyo Seikeigeka. 2005;40(1):13–7 (Japan).
16 Muhle C, Wiskirchen J, Weinert D, Falliner A, Wesner F, Brinkmann G, *et al.* Biomechanical aspects of the subarachnoid space and cervical cord in healthy indivisuals examined with kinematic magnetic resonance imaging. Spine 1998;23(5):556–67.
17 Muhle C, Metzner J, Weinert D, Falliner A, Brinkmann G, Mehdorn MH, *et al.* Classification system based on kinematic MR imaging in cervical spomdylotic myelopathy. AJNR 1998;19(9):1763–71.
18 Kato Y, Kataoka H, Ichihara K, Imajo Y, Kojima T, Kawano S, *et al.* Biomechanical study of cervical flexion myelopathy using a three-dimensional finite element method. J Neurosurg Spine 2008;8(5):436–41.
19 Kato Y, Kanchiku T, Imajo Y, Ichihara K, Kawano S, Hamanaka D, *et al.* Flexion model simulating spinal cord injury without radiographic abnormality in patients with ossification of the longitudinal ligament: the influence of flexion speed on the cervical spine. J Spinal Cord Med 2009;32(5):555–9.
20 Kato Y, Kanchiku T, Imajo Y, Kimura K, Ichihara K, Kawano S, *et al.* Biomechanical study of the effect of the degree of static compression of the spinal cord in ossification of the posterior longitudinal ligament. J Neurosurg Spine 2010;12(3):301–5.
21 Xin-Feng Li, MSc T, Li-Yang Dai. Three-dimensional finite element model of the cervical spinal cord. Spine 2009;34(11):1140–7.
22 Xin-Feng Li, MSc T, Li-Yang Dai. Acute central cord syndrome. Spine 2010;35(19):E955–E964.
23 Nishida N, Kato Y, Imajo Y, Kawano S, Taguchi T. Biomechanical study of the spinal cord in thoracic ossification of the posterior longitudinal ligament. J Spinal Cord Med 2011;34(5):518–22.
24 Henderson FC, Geddes JF, Vaccaro AR, Woodard E, Berry KJ, Benzel EC, *et al.* Stretch-associated injury in cervical spondylotic myelopathy: new concept and review. Neurosurgery 2005;56(5): 1101–13
25 Ono K, Ota H, Tada K, Yamamoto T. Cervical myelopathy secondary to multiple spondylotic protrusions: a clinicopathologic study. Spine 1977;2(2):109–25.
26 Ogino H, Tada K, Okada K, Yonenobu K, Yamamoto T, Ono K, *et al.* Canal diameter, anteroposterior compression ration, and spondylotic myelopathy of the cervical spine. Spine 1983;8(1):1–15.

J Orthop Sci (2012) 17:667–672
DOI 10.1007/s00776-012-0271-3

ORIGINAL ARTICLE

Perioperative complications of anterior cervical decompression with fusion in patients with ossification of the posterior longitudinal ligament: a retrospective, multi-institutional study

Atsushi Kimura · Atsushi Seichi · Yuichi Hoshino · Masashi Yamazaki · Macondo Mochizuki · Atsuomi Aiba · Tsuyoshi Kato · Kenzo Uchida · Kei Miyamoto · Shinnosuke Nakahara · Shinichirou Taniguchi · Masashi Neo · Toshihiko Taguchi · Kenji Endo · Masahiko Watanabe · Masahito Takahashi · Takashi Kaito · Hirotaka Chikuda · Takahito Fujimori · Takui Ito · Atsushi Ono · Kuniyoshi Abumi · Kei Yamada · Yukihiro Nakagawa · Yoshiaki Toyama

Received: 19 February 2012 / Accepted: 11 July 2012 / Published online: 10 August 2012

Abstract
Background Anterior decompression with fusion (ADF) for patients with cervical ossification of the posterior longitudinal ligament (OPLL) is reportedly associated with a higher incidence of complications than is laminoplasty. However, the frequency of perioperative complications associated with ADF for cervical OPLL has not been fully established. The purpose of this study was to investigate the incidence of perioperative complications, especially neurological complications, following ADF performed to relieve compressive cervical myelopathy due to cervical OPLL.
Methods Study participants comprised 150 patients who had undergone ADF for cervical OPLL at 27 institutions between 2005 and 2008. Perioperative—especially neurological—complications occurring within 2 weeks after ADF were analyzed. Preoperative imaging findings, including Cobb angle, between C2 and C7 and occupying ratio of OPLL were investigated. Multivariate analysis with logistic regression was performed to identify independent risk factors for neurological complications.

A. Kimura · A. Seichi (✉) · Y. Hoshino
Department of Orthopaedics, Jichi Medical University,
3311-1 Yakushiji, Shimotsuke, Tochigi 329-0498, Japan
e-mail: seichi-spine@jichi.ac.jp

M. Yamazaki
Department of Orthopaedic Surgery,
Chiba University Graduate School of Medicine,
1-8-1 Inohana, Chuo-ku,
Chiba 260-8670, Japan

M. Mochizuki · A. Aiba
Department of Orthopaedic Surgery, Numazu City Hospital,
550 Higashishiiji Azaharunoki, Numazu 410-0302, Japan

T. Kato
Department of Orthopaedic Surgery,
Tokyo Medical and Dental University,
1-5-45 Yushima, Bunkyo-ku, Tokyo 113-8519, Japan

K. Uchida
Department of Orthopaedics and Rehabilitation Medicine,
Faculty of Medical Sciences, University of Fukui,
Matsuoka Shimoaizuki 23-3, Eiheiji, Fukui 910-1193, Japan

K. Miyamoto
Department of Orthopaedic Surgery, Gifu University
School of Medicine, 1-1 Yanagido, Gifu 501-1194, Japan

S. Nakahara
Department of Orthopaedic Surgery,
National Okayama Medical Center,
1711-1 Tamasu, Kita-ku, Okayama 701-1192, Japan

S. Taniguchi
Department of Orthopaedic Surgery, Kochi Medical School,
185-1 Oko-cho Kohasu, Nankoku 783-8505, Japan

M. Neo
Department of Orthopaedic Surgery,
Graduate School of Medicine,
Kyoto University 54 Kawahara-cho Shogoin,
Sakyo-ku, Kyoto 606-8507, Japan

T. Taguchi
Department of Orthopaedic Surgery,
Yamaguchi University School of Medicine,
1-1-1 Minami-Kogushi, Ube, Yamaguchi 755-8505, Japan

K. Endo
Department of Orthopaedic Surgery, Tokyo Medical University,
6-7-1 Nishi-Shinjuku, Shinjuku-ku, Tokyo 160-0023, Japan

M. Watanabe
Department of Orthopaedic Surgery, Surgical Science,
Tokai University School of Medicine, 143 Shimokasuya,
Isehara, Kanagawa 259-1193, Japan

Result Three patients (2.0 %) showed deterioration of lower-extremity function after ADF. One of the three patients had not regained their preoperative level of function 6 months after surgery. Upper-extremity paresis occurred in 20 patients (13.3 %), five of whom had not returned to preoperative levels 6 months after surgery. Patients with upper-extremity paresis showed significantly higher occupying ratios of OPLL, greater blood loss, longer operation times, fusion of more segments, and higher rates of cerebrospinal fluid leakage than those without paresis. Independent risk factors for upper-extremity paresis were a high occupying ratio of OPLL and large blood loss during surgery.
Conclusions The incidences of deterioration in upper- and lower-extremity functions were 13.3 % and 2.0 %, respectively. Patients with a high occupying ratio of OPLL are at higher risk of developing neurological deterioration.

Introduction

Anterior decompression with fusion (ADF) is theoretically reasonable for treating cervical ossification of the posterior longitudinal ligament (OPLL), allowing direct removal of the ossified lesion. ADF has an advantage over posterior surgery in terms of spinal decompression, especially in patients with OPLL with a high canal-occupying ratio or kyphotic cervical alignment [1]. However, ADF for multisegmental OPLL is considered to be technically challenging and is reportedly associated with a higher incidence of surgery-related complications compared with laminoplasty [2]. Surgery-related complications include graft-bone migration [3], cerebrospinal fluid (CSF) leakage [4, 5], hoarseness, and neurological deficits [2, 5–8]. Despite this potential risk, the incidence of complications in patients with OPLL has not been fully established because of the relatively small number of patients included in previous studies [2, 7, 8]. We therefore investigated the incidence of perioperative complications associated with laminoplasty in patients with cervical OPLL in a multi-institutional retrospective study [9]. A subsequent multi-institutional study examined complications of ADF in patients with OPLL, during the same time period. The purpose of the study reported here was to investigate the incidence of perioperative complications, particularly neurological complications, following ADF performed to relieve compressive cervical myelopathy due to OPLL.

Methods

This study initially involved all cervical OPLL patients who had undergone ADF during the 3-year period from April 2005 to March 2008 at any one of the 27 participating institutions. All study protocols were approved by the institutional review board at the Japanese Society for Spine Surgery and Related Research. Questionnaires were sent to each institution in January 2009, and information on a total of 150 operated cases was collected. Patients who received ADF down to the first thoracic spine were included. Patients with traumatic spinal cord injury within 3 weeks of surgery and patients who had undergone simultaneous posterior cervical surgery or spinal surgery below T2 were excluded. Participants comprised 113 men and 37 women, with a mean age of 60 ± 10 (range 31–84) years.

M. Takahashi
Department of Orthopaedic Surgery, School of Medicine, Kyorin University, 6-20-2 Shinwaka, Mitaka, Tokyo 161-8611, Japan

T. Kaito
Department of Orthopaedic Surgery, National Hospital Organization Osaka Minami Medical Center, 2-1 Kidohigashimachi, Kawachinagano 586-8521, Japan

H. Chikuda
Department of Orthopaedic Surgery, Faculty of Medicine, The University of Tokyo, 7-3-1 Hongo, Bunkyo-ku, Tokyo 113-8655, Japan

T. Fujimori
Department of Orthopaedic Surgery, Osaka University Graduate School of Medicine, 2-2 Yamada-oka Suita, Osaka 565-0871, Japan

T. Ito
Department of Orthopedic Surgery, Niigata University Medical and Dental Hospital, Chuo-ku, Niigata 951-8510, Japan

A. Ono
Department of Orthopaedic Surgery, Hirosaki University School of Medicine, 5 Zaifu-cho, Hirosaki, Aomori 036-8562, Japan

K. Abumi
Department of Orthopaedic Surgery, Hokkaido University Graduate School of Medicine, Kita-15, Nishi-7 Kitaku, Sapporo 060-8638, Japan

K. Yamada
Department of Orthopaedic Surgery, Kurume University School of Medicine, 67 Ashahi-machi, Kurume 830-0011, Japan

Y. Nakagawa
Department of Orthopedic Surgery, Wakayama Medical University, 811-1 Kimiidera, Wakayama 641-8510, Japan

Y. Toyama
Department of Orthopaedic Surgery, School of Medicine, Keio University, 35 Shinanomachi, Shinjuku, Tokyo 160-8582, Japan

Clinical data

OPLL type was determined to be continuous in 15 patients, segmental in 53, mixed in 58, and local in 24 [10]. Items investigated were demographic data, imaging studies (X-ray, computed tomography, magnetic resonance imaging), surgical methods of decompression (complete resection of the ossified ligament or floating method), perioperative complications, and surgical outcome 6 months after surgery. Cobb angle between C2 and C7 (cervical lordotic angle; C2/7 angle) and occupying ratio of OPLL were also investigated. Spinal fusion involving a single disc level was defined as one fused segment and fusion of ≥ 3 segments was defined as a long fusion. Postoperative neurological complications within 2 weeks after ADF were described in detail. The type of postoperative upper-extremity paresis was categorized into proximal, distal, and diffuse type [11]. Outcomes were assessed by motor function scores of the upper and lower extremities for cervical myelopathy, as defined by the Japanese Orthopedic Association (JOA).

Statistical analysis

All statistical analyses were performed using SPSS version 17 software (SPSS, Chicago, IL, USA). Patients with motor function deterioration after surgery were compared with those without deterioration by univariate analysis using Mann–Whitney U tests for continuous variables and χ^2 tests for categorical variables. Multiple logistic regression analysis was used to identify independent risk factors using factors identified as significant by univariate analysis. A $P < 0.05$ was considered to be statistically significant.

Results

Demographic and surgical characteristics obtained from 21 institutes of the 150 patients are shown in Table 1. Slightly more than a quarter as many patients underwent ADF compared with the number in the previous study who underwent laminoplasty during the same time period (150 ADF vs. 581 laminoplasty) [9]. The number of cases of ADF at each institute ranged from 0 to 35. Although participating institutes are the main hospitals in local areas of the country, seven had no cases of ADF during the study period. Intraoperative spinal cord monitoring was implemented at only one of the 21 institutes. The preoperative JOA scores for lower-extremity function were 4 in 36 patients, 3 in 25, 2 in 52, 1 in 31, and 0 in 6. Those for upper-extremity function were 4 in 18 patients, 3 in 59, 2 in 47, 1 in 21, and 0 in 5.

The method of decompression was complete ossification resection in 106 (70.7 %) patients and use of the floating method in 44 (29.3 %) patients. Internal fixation of the cervical spine using a plate and screws was performed in 89 (59.3 %) patients, and the halo vest was applied in 26 (17.3 %). The incidence of bone-graft displacement did not differ significantly between patients with and without internal fixation or patients with and without halo vest. Perioperative complications other than neurological complications were CSF leakage in 22 (14.7 %), bone graft displacement in eight (5.3 %), and hoarseness in seven (4.6 %) patients. No patient experienced dyspnea or dysphagia after ADF. There was no significant difference in the incidence of CSF leakage between methods. All patients with bone graft displacement underwent revision surgery within 7 weeks; all patients who experienced hoarseness recovered spontaneously within 6 months.

Twenty patients (13.3 %) showed some form of neurological deterioration within 2 weeks following ADF (Table 2), all of whom showed deterioration of upper-extremity function. The onset upper-extremity function deterioration ranged from 0–10 (median 1) days. Types of paresis were classified as proximal (C5 palsy) in 14 patients, distal in three, and diffuse in three. Paresis generally improved in most patients, but five still showed poorer upper-extremity function 6 months after ADF compared with their preoperative level. Lower-extremity function deterioration was seen in three patients (2.0 %), the possible causes of which in one patient were assumed to be incomplete decompression and malalignment of the cervical spine. The patient underwent revision surgery to

Table 1 Demographics and surgical characteristics of the 150 patients

Characteristics	Data
Age (range)*	60 ± 10 (31–84)
Gender (male:female)	113:37
Occupying rate of OPLL (%)*	44.6 ± 16.2
Type of OPLL (%)	
Continuous	15 (10)
Mixed	58 (39)
Segmental	53 (35)
Localized	24 (16)
No. of fused segments (%)	
1	36 (24)
2	47 (31)
3	34 (23)
4	30 (20)
5	3 (2)
Operative time (min)*	271.2 ± 123.2
Blood loss (g)*	287.5 ± 564.5

* Mean ± standard deviation

OPLL ossification of the posterior longitudinal ligament

Table 2 Data for patients with neurological deterioration

No.	Age/ gender	Surgical levels	Occupying rate (%)	Onset (days)	Type of upper-extremity paresis	Concomitant lower-extremity paresis	Motor JOA score (upper/ lower)		Recovery of upper-extremity paresis	Recovery of lower-extremity paresis
							Preop	Postop. 6 M		
1	58/M	C3–C6	63.7	1	Proximal	Yes	3/2	3/2	Complete	Complete
2	52/F	C3–C6	92.0	1	Diffuse	Yes	0/1	3/1	Complete	Complete
3	58/M	C4–C7	58.9	1	Distal	Yes	3/2	2/1	Incomplete	Incomplete
4	58/F	C4–C7	N/A[a]	7	Diffuse	No	2/2	3/3	Complete	N/A
5	61/M	C4–C6	53.8	1	Proximal	No	3/4	4/4	Complete	N/A
6	75/M	C3–C4	63.6	2	Proximal	No	3/3	3/4	Complete	N/A
7	68/M	C4–C5	40.0	1	Proximal	No	3/4	4/4	Complete	N/A
8	62/M	C2–C6	50.0	0	Proximal	No	2/2	4/3	Incomplete	N/A
9	63/M	C4–C7	20.1	3	Proximal	No	2/4	4/4	Incomplete	N/A
10	71/M	C3–C5	46.2	1	Diffuse	No	2/1	2/1	Complete	N/A
11	66/M	C2–C6	45.0	2	Proximal	No	2/3	2/2	Complete	N/A
12	65/M	C3–C7	70.0	10	Proximal	No	1/1	2/2	Complete	N/A
13	68/M	C3–C7	38.5	1	Distal	No	3/1	3/1	Complete	N/A
14	58/M	C4–C7	54.8	1	Distal	No	3/2	3/4	Complete	N/A
15	53/M	C3–C6	50.0	1	Proximal	No	3/2	4/2	Complete	N/A
16	69/F	C3–C5	67.0	2	Proximal	No	3/3	3/3	Complete	N/A
17	76/M	C3–C6	83.0	3	Proximal	No	3/2	3/3	Incomplete	N/A
18	44/M	C4–C5	44.7	4	Proximal	No	1/4	2/4	Complete	N/A
19	54/M	C2–C5	36.2	1	Proximal	No	4/2	4/2	Incomplete	N/A
20	54/F	C2–C6	51.4	1	Proximal	No	3/2	3/3	Complete	N/A

JOA Japanese Orthopaedic Association, *Preop.* preoperative, *Postop.* postoperative

[a] Occupying rate was not applicable due to a preceding laminoplasty

correct the problem 19 days after surgery. Although lower-extremity function subsequently improved in this patient, it had still not recovered to the preoperative level at 6 months after surgery. No obvious cause of deterioration was identified in the other two patients with deterioration of lower-extremity function; however, both showed spontaneous improvement, and lower-extremity function had returned to preoperative levels by 6 months after surgery. The decompression method was complete ossification resection in all of three patients with neurological deterioration.

Patient data, including occupying ratio, C2/7 angle, long fusion (≥3 fused segments), blood loss, operative time, surgical method of decompression, and CSF leakage, were compared between patients with and without upper-extremity paresis. Significant factors in univariate analysis were occupying ratio, blood loss, operative time, long fusion, and CSF leakage (Table 3). Multivariate analysis using logistic regression was subsequently performed to identify independent risk factors for deterioration of upper-extremity function. Significant independent risk factors for upper-extremity paresis were occupying ratio and blood loss (Table 4). High OPLL occupying ratio was the only identified risk factor that could be identified by preoperative imaging studies.

Discussion

The frequency of perioperative complications following ADF in patients with OPLL has largely been investigated in small case series only because of the relatively low prevalence of OPLL [12] and the limited indications for ADF in patients with multisegmental OPLL [2]. This means that there is insufficient information regarding the risk of complications to allow patients with OPLL to make appropriately informed choices. This study investigated the incidence of perioperative complications based on retrospective analysis of data from numerous institutions. Multivariate analysis revealed that patients with a high occupying ratio of OPLL are at increased risk of developing neurological deterioration after ADF.

Table 3 Univariate comparisons of individual risk factors in patients with and without upper-extremity paresis following ADF

Risk factors	Patients with upper-extremity paresis[a] ($N = 20$)	Patients without upper-extremity paresis[a] ($N = 130$)	Odds ratio (95 % confidence interval)	P value
Occupying ratio (%)	54.2 ± 16.8	43.1 ± 15.7	Not applicable	0.005
C2/7 angle (degree)	7.2 ± 9.9	8.8 ± 10.4	Not applicable	0.758
Blood loss (g)	729.7 ± 1367.5	218.4 ± 231.4	Not applicable	0.021
Operative time (min)	351.4 ± 26.7	258.7 ± 10.6	Not applicable	0.002
Long fusion (no. of fused segments ≥3)	14 (70 %)	53 (41 %)	3.39 (1.224–9.385)	0.017
CSF leakage	7 (35 %)	15 (12 %)	3.84 (1.333–11.045)	0.016

ADF anterior decompression with fusion, *CSF* cerebrospinal fluid

[a] Values are given as mean ± standard deviation for continuous variables and as number of patients, with the percentage in parentheses, for categorical variables. Continuous variables were analyzed using Mann–Whitney U tests, and categorical variables were analyzed using χ^2 tests

Table 4 Multivariate logistic regression model for the development of upper-extremity paresis following ADF

Risk factor	Odds ratio (95 % confidence interval)	P value
Occupying ratio	1.047 (1.002–1.093)	0.040
Blood loss	1.002 (1.000–1.003)	0.047
Operative time	1.001 (0.996–1.006)	0.737
Long fusion	0.827 (0.230–2.982)	0.772
CSF leakage	0.337 (0.960–1.188)	0.091

ADF anterior decompression with fusion, *CSF* cerebrospinal fluid

Deterioration of lower-extremity function, including quadriplegia, is one of the most critical complications following spine surgery. However, few studies have focused on the incidence of deterioration of lower-extremity function following ADF in patients with cervical OPLL. Also, the reported incidence varies among studies from 0 % to 14.3 % [2, 7, 8] because of the small numbers of patients assessed in each study. The study reported here found an incidence of 2.0 % (3/150 patients), which was comparable with the 3.1 % following laminoplasty determined in our previous study [9]. Given that one of the three patients with deterioration had not regained preoperative functional level 6 months after surgery, the potential risk of paralysis in the lower extremity should be included in the informed consent information provided to patients before the surgical procedure.

Several relatively large case series investigated the incidence of upper-extremity palsy, especially fifth cervical nerve (C5) palsy, following ADF. The reported incidence of C5 palsy ranges from 2.4 % to 8.5 % [6, 13, 14], although these results were largely obtained in patients with cervical spondylotic myelopathy (CSM). The incidence of upper-extremity function deterioration in this study was 13.3 %, which is higher than in previous studies. This higher incidence could be attributable to several factors. First, our results included paresis of cervical nerves other than C5 (C6, C7, or C8), which are described as distal type or diffuse type [11], whereas upper-extremity paresis confined to the C5 area occurred in only 9.3 % (14/150 patients) in our series. Second, our study group consisted exclusively of patients with OPLL. Several studies demonstrated slightly higher incidences of C5 palsy in patients with OPLL compared with those in patients with CSM following ADF [6, 13], although the reasons for this higher incidence have not been clarified.

Possible mechanisms responsible for neurological deterioration include iatrogenic damage to the spinal cord during the decompression procedure, tethering or kinking of the nerve root caused by anterior shift of the spinal cord [13], reperfusion injury of the ischemic spinal cord [14], displacement of graft bone [3], and epidural hematoma. Almost no specific cause of neurological deterioration was identified in this series. However, considering that high canal-occupying ratio and large blood loss were identified as independent risk factors for neurological deterioration, the deterioration may be partly caused by iatrogenic damage to the spinal cord or nerve roots during the decompression procedure as a result of poor visualization of the surgical site due to bleeding.

In this study, patients with neurological deterioration showed significantly higher rates of CSF leakage than those without deterioration, although CSF leakage was not identified as an independent risk factor for deterioration in multivariate analysis. Given that OPLL with a high occupying ratio shows an increased rate of dural ossification, which is a predisposing factor for CSF leakage during anterior resection of the lesion [15, 16], CSF leak may be indirectly related to deterioration in high-space-occupying lesions with dural ossification. Even though CSF leakage was not identified as an independent risk factor for neurological deterioration, it should be avoided whenever possible to prevent troublesome sequelae, such as cutaneous fistula, respiratory obstruction, and pseudomeningocele [4].

Limitations of this study include the variability in number of cases among institutes and its retrospective nature. The difference in numbers of patients from each institution, ranging from 0 to 35, suggests that surgical indication, as well as surgeon experience with ADF in patients with OPLL, varied. Although the number of cases treated at each institute was not significantly correlated with neurological deterioration (data not shown), our results should be interpreted with caution. No statistical comparison between ADF and laminoplasty was performed because patients' backgrounds, including age, JOA score, and C2/7 angle, differed significantly between groups. Another limitation is that the rate of microsurgical decompression remains unclear. The use of a microscope is suggested to be essential for performing a less traumatic decompression procedure [8]. Moreover, the incidence of pseudoarthrosis needs to be elucidated in future study because it is an important complication following ADF.

In conclusion, this retrospective, multi-institutional study revealed that ADF in patients with cervical OPLL is associated with a risk of neurological complications. The incidence of deterioration in upper- and lower-extremity function was 13.3 % and 2.0 %, respectively. Patients with a high occupying ratio of OPLL are at an increased risk of developing neurological deterioration. Patients with OPLL who undergo ADF should be properly informed of the potential risks of neurological deterioration, despite its usually transient nature in the majority of patients.

Acknowledgments This work was supported by a Health Labour Sciences Research Grant. No benefits in any form have been or will be received from any commercial party related directly or indirectly to the subject of this article.

References

1. Fujiyoshi T, Yamazaki M, Kawabe J, Endo T, Furuya T, Koda M, Okawa A, Takahashi K, Konishi H. A new concept for making decisions regarding the surgical approach for cervical ossification of the posterior longitudinal ligament: the K-line. Spine. 2008;33:E990–3.
2. Iwasaki M, Okuda S, Miyauchi A, Sakaura H, Mukai Y, Yonenobu K, Yoshikawa H. Surgical strategy for cervical myelopathy due to ossification of the posterior longitudinal ligament: part 2: advantages of anterior decompression and fusion over laminoplasty. Spine. 2007;32:654–60.
3. Wang JC, Hart RA, Emery SE, Bohlman HH. Graft migration or displacement after multilevel cervical corpectomy and strut grafting. Spine. 2003;28(1016–21):21–2.
4. Mazur M, Jost GF, Schmidt MH, Bisson EF. Management of cerebrospinal fluid leaks after anterior decompression for ossification of the posterior longitudinal ligament: a review of the literature. Neurosurg Focus. 2011;30:E13.
5. Cardoso MJ, Koski TR, Ganju A, Liu JC. Approach-related complications after decompression for cervical ossification of the posterior longitudinal ligament. Neurosurg Focus. 2011;30:E12.
6. Ikenaga M, Shikata J, Tanaka C. Radiculopathy of C-5 after anterior decompression for cervical myelopathy. J Neurosurg Spine. 2005;3:210–7.
7. Jain SK, Salunke PS, Vyas KH, Behari SS, Banerji D, Jain VK. Multisegmental cervical ossification of the posterior longitudinal ligament: anterior vs posterior approach. Neurol India. 2005;53:283–5; discussion 6.
8. Tani T, Ushida T, Ishida K, Iai H, Noguchi T, Yamamoto H. Relative safety of anterior microsurgical decompression versus laminoplasty for cervical myelopathy with a massive ossified posterior longitudinal ligament. Spine. 2002;27:2491–8.
9. Seichi A, Hoshino Y, Kimura A, Nakahara S, Watanabe M, Kato T, Ono A, Kotani Y, Mitsukawa M, Ijiri K, Kawahara N, Inami S, Chikuda H, Takeshita K, Nakagawa Y, Taguchi T, Yamazaki M, Endo K, Sakaura H, Uchida K, Kawaguchi Y, Neo M, Takahashi M, Harimaya K, Hosoe H, Imagama S, Taniguchi S, Ito T, Kaito T, Chiba K, Matsumoto M, Toyama Y. Neurological complications of cervical laminoplasty for patients with ossification of the posterior longitudinal ligament-a multi-institutional retrospective study. Spine. 2011;36:E998–1003.
10. Hirabayashi K, Miyakawa J, Satomi K, Maruyama T, Wakano K. Operative results and postoperative progression of ossification among patients with ossification of cervical posterior longitudinal ligament. Spine. 1981;6:354–64.
11. Seichi A, Takeshita K, Kawaguchi H, Nakajima S, Akune T, Nakamura K. Postoperative expansion of intramedullary high-intensity areas on T2-weighted magnetic resonance imaging after cervical laminoplasty. Spine. 2004;29:1478–82; discussion 82.
12. McAfee PC, Regan JJ, Bohlman HH. Cervical cord compression from ossification of the posterior longitudinal ligament in non-orientals. J Bone Joint Surg Br. 1987;69:569–75.
13. Sakaura H, Hosono N, Mukai Y, Ishii T, Yoshikawa H. C5 palsy after decompression surgery for cervical myelopathy: review of the literature. Spine. 2003;28:2447–51.
14. Hasegawa K, Homma T, Chiba Y. Upper extremity palsy following cervical decompression surgery results from a transient spinal cord lesion. Spine. 2007;32:E197–202.
15. Chen Y, Guo Y, Chen D, Lu X, Wang X, Tian H, Yuan W. Diagnosis and surgery of ossification of posterior longitudinal ligament associated with dural ossification in the cervical spine. Eur Spine J. 2009;18:1541–7.
16. Mizuno J, Nakagawa H, Matsuo N, Song J. Dural ossification associated with cervical ossification of the posterior longitudinal ligament: frequency of dural ossification and comparison of neuroimaging modalities in ability to identify the disease. J Neurosurg Spine. 2005;2(425–30):17.

Spine

SPINE Volume 37, Number 5, pp E309–E314

SRS Focus Issue

Ossification of the Posterior Longitudinal Ligament of the Cervical Spine

Etiology and Natural History

Shunji Matsunaga, MD, PhD, and Takashi Sakou, MD, PhD

Study Design. Review article.

Objective. To review the etiology, natural history, measurement tools, and image diagnosis of ossification of the posterior longitudinal ligament (OPLL) of the cervical spine.

Summary of Background Data. OPLL is a well-known disease that causes myelopathy. Genetic factors are very important for development of OPLL. However, the pathogenetic gene and natural history of OPLL have not been clarified.

Methods. The authors reviewed studies about the etiology, natural history, measurement tools, and diagnosis of OPLL, which had been performed by the members of the Investigation Committee on the Ossification of the Spinal Ligaments of the Japanese Ministry of Health, Labour, and Welfare.

Results. The prevalence of OPLL in the general Japanese population was reported to be 1.9% to 4.3% among people older than 30 years. Genetic factors are important for development of OPLL, and some candidate genes have been reported. Clinical course of OPLL has been clarified by a prospective long-term follow-up study. Some radiographic predictors for development of myelopathy were introduced. Image diagnosis of OPLL is easy by plain radiographs, but magnetic resonance imaging and computed tomography are useful to determine cord compression by OPLL.

Conclusion. OPLL should be managed on the basis of the consideration of its natural history. Elucidation of pathogenetic genes of OPLL will introduce a new approach for management of OPLL.

Key words: ossification of the posterior longitudinal ligament (OPLL), pathogenetic gene, prevalence of OPLL, natural course of OPLL. **Spine 2012;37:E309–E314**

From the Imakiire General Hospital, Kagoshima, Japan.

Acknowledgment date: January 10, 2011. Acceptance date: September 28, 2011.

The manuscript submitted does not contain information about medical device(s)/drug(s).

The Investigation Committee on the Ossification of the Spinal Ligaments of the Japanese Ministry of Health, Labour, and Welfare funds were received in support of this work.

No benefits in any form have been or will be received from a commercial party related directly or indirectly to the subject of this manuscript.

Address correspondence and reprint requests to Shunji Matsunaga, MD, PhD, Imakiire General Hospital, 4–16 Shimotatsuo chou, Kagoshima 892–8502, Japan; E-mail: shunji@m.kufm.kagoshima-u.ac.jp

DOI: 10.1097/BRS.0b013e318241ad33

Ossification of the posterior longitudinal ligament (OPLL) is a hyperostotic condition of the spine associated with severe neurologic deficit.[1,2] This disease was first reported about 160 years ago.[3] OPLL was previously considered specific to Asian people and did not attract attention in Europe or the United States. However, OPLL has come to be recognized as a subtype of diffuse idiopathic skeletal hyperostosis,[4,5] which is well known in Europe and the United States. We summarize the prevalence of OPLL and clinical findings regarding this unique entity.

ETIOLOGY

Prevalence

OPLL was found to occur in 1.5% to 2.4% of adult outpatients with cervical disorders at several university hospitals in Japan (Table 1).[6] In the same survey of foreign countries, the prevalence of OPLL was 0.4% to 3.0% in Asian countries (Table 2). The incidence of OPLL in the general Japanese population was reported to be 1.9% to 4.3% among people older than 30 years (Table 3). In 1992, Epstein[30] proposed a new concept about OPLL. Epstein[30] examined computed tomographic (CT) scans of the cervical spine in whites and noted hypertrophy of the posterior longitudinal ligament with punctuate calcification. This finding was described as OPLL in evolution.[31] Epstein[31] noted that the prevalence of OPLL among whites with cervical myelopathy has recently increased from 2% to 25%.

Genetic Study

A genetic survey of OPLL patients has revealed a higher rate of occurrence among families. A nationwide survey in Japan of 347 families of patients with OPLL revealed that OPLL was radiographically detected in 24% of the second-degree or closer blood relatives and in 30% of OPLL patients' siblings.[32] A nationwide study in Japan by the committee, including 10 sets of twins (8 monozygotic twin pairs and 2 dizygotic twin pairs) who exhibited OPLL, was performed. Six of the 8 monozygotic twin pairs had OPLL. This suggested or implicated a genetic factor contributing to the frequency of this disease among the twins. A human leukocyte antigen (HLA) haplotype analysis provides a useful means for

TABLE 1. OPLL in Outpatient Clinic for Cervical Disorders in Japan

	Location of Survey	Subjects (n)	Age of Subjects (yr)	OPLL (n)	Incidence of OPLL (%)
Okamoto 1967[7]	Okayama	1000	ND	21	2.1
Yanagi *et al* 1977[8]	Nagoya	1300	>20	31	2.4
Onji *et al* (1967)[9]	Osaka	1800	ND	31	1.7
Shinoda *et al* 1971[10]	Sapporo	3747	>10	55	1.5
Harata 1976[11]	Hirosaki	2275	ND	33	1.5
Sakou *et al* 1978[12]	Okinawa	1969	>30	30	1.5
Kurihara *et al* 1978[13]	Kobe	9349	>15	183	2.0
Izawa 1980[14]	Tokyo	6944	>20	143	2.1

ND indicates not determined; OPLL, ossification of the posterior longitudinal ligament.

Reprinted with permission from Yonenobu et al. *OPLL. Tokyo, Japan: Springer–Verlag; 1997:13.*

studying genetic backgrounds of diseases and was performed in patients with OPLL. HLA is the name of the major histocompatibility complex in humans. The super locus contains a large number of genes related to immune system function in humans. An HLA haplotype is a series of HLA "genes" (loci-alleles) by chromosome, 1 passed from the mother and 1 from the father. HLA haplotypes can be used to trace migrations in the human population. Specific HLA haplotype of OPLL could not be found in this study, but a very interesting finding was that if a sibling had both the same haplotypes as the proband, the prevalence of OPLL was much higher than if the sibling had only 1 of the same haplotypes as the proband. If neither of the haplotypes was seen in the proband, the occurrence was almost nil (Table 4).[33,34] Some candidate genes *(collagen α2 [XI],*[35,36] *collagen 6A1*[37] *human nucleotide pyrophosphatase [NPPS]* gene[38,39]) for OPLL were reported. *Collagen α2 (XI)* is a human gene that is 1 of the several genes that provide instructions for the production of type XI collagen. The *collagen α2 (XI)* gene produces 1 component of this type of collagen, called the pro-α2(XI) chain. Type XI collagen adds structure and strength to the tissues that support the connective tissue. Collagen VI is a major structural component of microfibrils. Collagen α-1 (VI) chain is a protein that, in humans, is encoded by the *COL6A1* gene. The collagen is a superfamily of proteins that play a role in maintaining the integrity of various tissues. *NPPS*, a membrane-bound

TABLE 2. OPLL in Outpatient Clinic in the World

	Reporter	Country	Subjects (n)	Age of Subjects (yr)	OPLL (n)	Incidence of OPLL (%)
Asia	Yamauchi 1978[15]	Korea	529	>20	5	1.0
	Kurokawa 1978[16]	Taiwan	395	>40	12	3.0
		Hong Kong	498	>40	2	0.4
	Yamaura *et al* 1978[17]	Philippine	332	ND	5	1.5
	Tezuka 1980[18]	Taiwan	661	>20	14	2.1
	Lee *et al* 1991[19]	Singapore	5167	>30	43	0.8
Europe & United States	Yamauchi *et al* 1979[20]	West Germany	1060	>27	1	0.1
	Terayama and Ohtsuka 1984[21]	Italy	1258	>35	22	1.7
	Izawa 1980[14]	Minnesota	840	>30	1	0.1
		Hawaii	490	>20	3	0.6
	Firooznia *et al* 1982[22]	New York	1000	>20	7	0.7
	Ijiri *et al* 1996[23]	Utah	599	>30	8	1.3

ND indicates not determined; OPLL, ossification of the posterior longitudinal ligament.

Reprinted with permission from Yonenobu et al. *OPLL. Tokyo, Japan: Springer–Verlag; 1997:13.*